Nuclear magnetic resonance and surface-assisted laser desorption/ionization mass spectrometry-based metabolome profiling of urine samples from kidney cancer patients

Joanna Nizioł[a*], Krzysztof Ossoliński[b], Brian P. Tripet[c], Valérie Copié[c], Adrian Arendowski[a] and Tomasz Ruman[a]

[a]*Rzeszów University of Technology, Faculty of Chemistry, 6 Powstańców Warszawy Ave., 35-959 Rzeszów, Poland, e-mail: jniziol@prz.edu.pl*

[b]*Department of Urology, John Paul II Hospital, Grunwaldzka 4 St., 36-100 Kolbuszowa, Poland*

[c]*The Department of Chemistry and Biochemistry, Montana State University, Bozeman, Montana 59717, United States*

*Corresponding author: Joanna Nizioł, e-mail: jniziol@prz.edu.pl, tel: (+48 17) 865-1896

Abstract

Kidney cancer is one of the most frequently diagnosed cancers of the urinary tract in the world. Despite significant advances in kidney cancer treatment, no urine specific biomarker is currently used to guide therapeutic interventions. In an effort to address this knowledge gap, metabolic profiling of urine samples from 50 patients with kidney cancer and 50 healthy volunteers was undertaken using high-resolution proton nuclear magnetic resonance spectroscopy (^{1}H NMR) and silver-109 nanoparticle enhanced steel target laser desorption/ionization mass spectrometry (^{109}AgNPET LDI MS). Twelve potential urine biomarkers of kidney cancer were identified and quantified using one-dimensional (1D) ^{1}H NMR metabolomics. Seven mass spectral features which differed significantly in abundance ($p<0.05$) between kidney cancer patients and healthy volunteers were also detected using ^{109}AgNPET-based laser desorption/ionization mass spectrometry (LDI MS). This work provides a framework to expand biomarker discovery that could be used as useful diagnostic or prognostic of kidney cancer progression

Keywords: kidney, cancer, mass spectrometry, biomarkers, proton nuclear magnetic resonance , urine

1. Introduction

Kidney cancer is among the 15 most commonly occurring cancers worldwide in terms of incidence and mortality in both men and women. More than 400,000 new kidney cancer cases and nearly 180,000 deaths were recorded in 2018. Kidney cancer is not a single disease, as there exists a number of different types of kidney tumors which differ in histology, responses to therapy, and progression to different clinical outcomes. Kidney tumors can be benign, indolent, or malignant. Non-cancerous tumors include adenoma, oncocytoma and angiomyolipoma (AML). Renal cell carcinoma (RCC) is the most common and malignant type of kidney cancer accounting for approximately 90% of all neoplasms arising from the kidney. There are three main types of RCC including clear cell (ccRCC), papillary RCC (pRCC) and chromophobe RCC (cRCC) that differ in their stage, grade, and cancer-specific survival. Subtypes of RCC such as angiomyolipoma (AML), collecting duct carcinoma (CDC), or simple renal cyst (SRC) are very rare [1].

Currently, kidney cancer diagnosis is based on abdominal ultrasound, magnetic resonance imaging, or computed tomography; however, more than 60% of RCCs are diagnosed incidentally when patients are examined for other reasons. Kidney cancer is one of the few cancers whose occurrence is increasing every year. In most cases, RCC progresses asymptomatically, and is difficult to detect at an early stage due to the lack of characteristic symptoms such as classic triad of visible haematuria, flank pain and palpable abdominal mass symptoms [2].

Unfortunately, though great efforts have been dedicated in the past decades to identify characteristic small molecule indicators of kidney cancer, there are currently no reliable biomarkers available to guide more effective therapies, diagnosis, or disease prognosis. Therefore, further research and the development of new kidney cancer sensitive biomarkers are of great importance, not only to improve prognosis, early detection as well as to monitor treatment, but also to enhance our understanding of the molecular processes underlying kidney cancer, using preferably non-invasive methods [3].

Over the past decades, the use of metabolomics applications to cancer research has increased significantly. Analysis of metabolite profiles from non-invasive sources such as biofluids is a promising approach for the discovery of valuable biomarkers to enhance our abilities to predict cancer progression, screen cancer pathologies, and to assess the effectiveness of cancer treatments. Urine is a preferred source of biospecimens for metabolomics analysis of kidney cancer due to its close association with disease origin. Urine metabolomes provide biochemical fingerprints of systemic changes in organisms, and an avenue to identify and characterize potential biomarkers associated with cancer, including kidney cancer [4]. The most frequently used techniques for metabolomic analysis of kidney cancer have been liquid chromatography-coupled mass spectrometry (LC-MS) [5], gas chromatography-coupled mass spectrometry (GC-MS) [6], and ^{1}H nuclear magnetic resonance (NMR) spectroscopy [7]. Since kidney cancer is recognized as a metabolomic disease, a growing number of studies focusing on the metabolite profiling of tissues [8] and biofluids from patients, including plasma [9], serum [10], and urine [11] have been reported.

MS-based methods have been some of the most prominent approaches utilized in untargeted metabolomic analyses of urine samples. In 2006, Perround et al. employed metabolomics techniques to characterize the urine metabolome of a small group of patients (5 RCC and 5 control), and to identify potential biomarkers of kidney cancer [12]. A similarly small group of RCC patients was examined a year later by the Weiss group, who employed three different analytical techniques to broaden the detection and coverage of urinary metabolites [13]. In 2011, Kim et al. utilized MS-based metabolomics to evaluate the differential levels of compounds present in the urine of 29 kidney cancer patients and 33 control patients. They found that measuring the differential concentrations of the three metabolites gentisate, quinolinate, and 4-hydroxybenzoate could be used successfully to distinguish RCC patients from controls [14]. In 2012, Ganti et al. analyzed the urine metabolome of 29 RCC and 33 control patients using LC-MS and GC-MS, and found that most acylcarnitines were increased in the urine of cancer patients, and that the concentrations of these compounds were dependent on both cancer status and kidney cancer grade [11]. In 2016, Monteiro et al. performed a metabolomic profiling analysis of urine from 42 RCC patients and 49 controls using NMR spectroscopy, and found 32 metabolites whose significantly altered levels between the two groups [15].

NMR-based metabolomic studies of urine samples from RCC patients are rarely reported in literature [16,17]. To our knowledge, there are no current studies that have combined both NMR and LDI MS approaches to conduct comprehensive analyses of the urine metabolome of patients with kidney cancer.

This work is the first to report on the metabolomics-based profiling of urine samples from patients with kidney cancer (n=50) and controls (n=50), using two orthogonal analytical methods: high resolution ^{1}H NMR and laser desorption/ionization mass spectrometry with 109-silver nanoparticle-enhanced steel target (^{109}AgNPET LDI MS) [18]. Results from this study have identified interesting small molecule candidate biomarkers, which may be useful to discriminate kidney cancer patients from healthy controls based on differential urine metabolome profiles.

2. Experimental section

2.1. Materials and equipment

^{109}AgNPET materials were prepared as described in our previous publication [19]. All solvents were of HPLC quality, except for methanol and water (LCMS grade, Fluka).

2.2. Patient characteristics

The protocol of this study was approved by local Bioethics Committee at the University of Rzeszow (Poland) (permission no. 2018/04/10). Authors confirm that all research was performed in accordance with relevant regulations and guidelines. Specimens and clinical data from patients involved in the study were collected with informed consent. Urine samples were obtained from fifty patients with kidney cancer and 50 age- and sex-matched healthy

control subjects, following detailed clinical questioning at the John Paul II Hospital in Kolbuszowa (Poland). Laboratory test results (complete blood count, kidney function tests, CRP, urine analysis, bleeding profile) were within normal ranges. Urine samples from 50 patients (20 female, 30 male, age range 36-87, average age 69) with kidney cancer and 50 healthy control subjects were collected. The majority of patients (n=33) had a disease stage of T1, four patients had T2 stages, ten patients had T3 stages, and one patient had a stage of T4. In three patients, the stage of the disease could not be determined. Among tumors diagnosed, there were 33 clear cell renal cell carcinomas (ccRCC), 4 oncocytomas, 4 angiomyolipomas (AML), 2 chromophobe renal cell carcinomas (chRCC), 2 papillary renal cell carcinomas (pRCC), 1 collecting duct carcinoma (CDC), 1 simple renal cyst (SRC) and 1 tubulocystic renal cell carcinoma (TCRC), classified according to the 2016 *WHO Classification of Tumors of the Urinary System and Male Genital Organs*. Most of the diagnosed cancers were malignant (n=41), but few patients (n=7) had benign (non-cancerous) kidney tumors. In this study, benign tumors of the kidney included oncocytoma and angiomyolipoma, while other types of tumors were considered malignant. In addition, one patient had a lung adenocarcinoma metastasis. The pathological and clinical characteristics of the patients are presented in supplementary material (Table S1).

2.3. Preparation of urine samples

A volume of 10 mL of urine was drawn from each participant. The urine was stored at –60ºC until further use. Prior to NMR analysis, urine samples were thawed at 4°C, then centrifuged at 12000xg for 5 min at 4°C to remove cells and other solid materials. A volume of 900 µL of acetone was added to 300 µL of resulting supernatants. After vortexing for 1 min, the solutions were incubated at room temperature for 20 min followed by 30 min at -20°C, and then centrifuged at 6000xg for 5 min at 4 °C. Next, 800 µL volumes of clarified supernatants were transferred to a new polypropylene tube. The pellets were re-suspended in 500 µl of acetone-H_2O mixture (3:1, v/v) and vortexed vigorously. Samples were subjected to centrifugation at 12000xg for 10 min at 4°C. The supernatants from pellet washes were combined with the supernatants from the first spin. Finally, from approx. 990 µl of resulting samples, 50 µl was taken and used for ^{109}AgNPET LDI MS analysis. The rest of the sample was dried to complete dryness using a SpeedVac vacuum concentrator (1 mbar vacuum, 24 hours), with no heating applied. Dried extracts were re-suspended in 600 µL of NMR buffer consisting of 25 mM NaH_2PO_4/Na_2HPO_4, 0.4 mM imidazole, 0.25 mM 4,4-dimethyl-4-silapentane-1-sulfonic acid (DSS) in 90% H_2O/10% D_2O, pH 7.0. Following re-suspension, samples were centrifuged at 21,000 rpm for 1 min to pellet insoluble debris, and then transferred to 5 mm NMR tubes for NMR metabolomics analysis.

2.4. NMR Spectra Acquisition and Preprocessing

1D ^{1}H NMR spectra were collected at Montana State University at 298 K (25°C), using a Bruker 600 MHz (^{1}H Larmor frequency) AVANCE III solution NMR spectrometer, equipped with a SampleJet automatic sample loading system, a 5 mm triple resonance (^{1}H, ^{15}N, ^{13}C), liquid-helium-cooled TCI NMR cryoprobe, and Topspin software (Bruker version 3.6). 1D ^{1}H NMR spectra acquisition was performed using the Bruker-supplied excitation

sculpting (ES)-based 'zgesgp' pulse sequence, and NMR spectra were recorded using 256 scans, a ^{1}H spectral window of 7211.538 Hz, 64K data points and a dwell time interval of 69.33 µsec between points, amounting to a spectrum acquisition time of 4.54 s. The recovery delay (D1) time between acquisitions was set to 2 s, resulting in a total relaxation recovery time of 6.5 s between scans. Chemical shift referencing using the DSS NMR signal and phase correction of 1D ^{1}H NMR spectra were conducted using the Topspin software (Bruker version 3.6), as detailed previously [20].

For validation of metabolite annotation, 2D ^{1}H-^{1}H total correlation spectroscopy (TOCSY) spectra were acquired for representative samples using the Bruker-supplied 'mlevphpr.2/mlevgpph19' pulse sequences (256 × 2048 data points, 2 s relaxation delay, 32 transients per FID, 1H spectral window of 6602.11 Hz, 80 ms TOCSY spin lock mixing period). 2D ^{1}H-^{1}H TOCSY spectra were processed using Topspin software (Bruker version 3.6).

2.5. NMR Data Analysis

Further processing of 1D ^{1}H NMR spectra and metabolite profiling analyses were conducted using the Chenomx NMR Suite software (version 8.1; Chenomx Inc., Edmonton, Alberta, Canada). Baseline correction of NMR spectra following import of preprocessed '1r' NMR spectral files into Chenomx software was performed using the automatic cubic spline function in Chenomx, and subsequent manual breakpoint adjustment to obtain a flat, well-defined baseline, following recommendations from Chenomx application notes and previously reported methods [20,21]. ^{1}H chemical shifts were referenced to the 0.0 ppm DSS signal, and the ^{1}H NMR signals arising from imidazole were used to correct for small chemical shift changes due to slight variations in sample pH. Metabolite identification and quantification were performed by fitting 1D ^{1}H spectral splitting patterns, chemical shifts, and spectral intensities to reference spectral patterns of small molecules, using the Chenomx small molecule spectral database for 600 MHz (^{1}H Larmor frequency) magnetic field strength NMR, and manually peak-based fits, where adjustments were made to achieve optimal spectral pattern fits for compound peak cluster location and intensity. The internal DSS standard (0.25mM) was used for metabolite quantitation.

2.6. MS Sample Preparation

0.3 µl of each sample was placed on a ^{109}AgNPET and allowed to dry at room temperature, followed by target insertion into a MALDI ToF/ToF mass spectrometer.

2.7. MS Spectra Acquisition and Preprocessing

Laser desorption ionization mass spectrometry imaging (LDI-MSI) experiments were performed using a Bruker Autoflex Speed time-of-flight mass spectrometer in positive-ion reflectron mode. The apparatus was equipped with a SmartBeam II 1000 Hz 355 nm laser, with a laser impulse energy of approximately 100−190 µJ, laser repetition rate of 1000 Hz, and deflection set on *m/z* lower than 80, with a *m/z* range of 80−2000 Da. Spectrum for each

extract contained data from 20k laser shots with a default random walk applied (random points with 50 laser shots). All spectra were calibrated with the use of silver ions ($^{109}Ag^+$ to $^{109}Ag_{10}^+$). The first accelerating voltage was held at 19 kV, and the second ion source voltage was held at 16.7 kV. Reflector voltages used were 21 kV (the first) and 9.55 kV (the second). FlexAnalysis 4.0 software was used for data processing and analysis.

2.8. Multivariate statistical analysis

Metabolite data was log-transformed and auto-scaled prior to statistical analysis, which was accomplished using the MetaboAnalyst software 4.0 [22].

Firstly, a total of 100 ^{1}H NMR and 100 LDI MS of recorded spectra were subjected to an unsupervised multivariate statistical analysis, Principal Component Analysis (PCA), to reveal whether distinct urine metabolic profiles can separate kidney cancer from healthy controls, and to detect possible outliers. The extent of the separation between these two groups was further examined using a supervised multivariate statistical analysis, Partial Least Squares Discriminant Analysis (PLS-DA).

The quality of PLS-DA model was described by predictability of the model (Q^2), goodness of fit (R^2), and accuracy (data permutation tests). Variable Importance in the Projection (VIP) plots were generated to focus on metabolites whose level changes most significantly contributed to the group separation. Metabolites with VIP scores > 1 were considered to be significant contributors, and potential biomarkers to distinguish kidney cancer patients from healthy controls. In this work, 10-fold cross validations were used to define the number of latent variables (PLS components) in the model. To test the accuracy of multivariate models, and minimize the possibility that the observed separation in the PLS-DA is due to chance ($p<0.05$), permutation tests were performed using 2000 repetition steps. Statistical significance of metabolite level differences was assessed using unpaired parametric t-test with Mann–Witney and Bonferroni correction. P values and false discovery rates (FDR; q-value) less than 0.05 were considered statistically significant. Additionally, receiver operating curve (ROC) analyses were conducted to evaluate the diagnostic value of selected metabolites. Standard chemometrics tools such as 2D PCA and PLS-DA analysis were also used to assess metabolic profile similarities and differences between cancer types (malignant and benign) and grades (grade 1, 2 and 3). An approximation was used whereby all malignant renal tumors like ccRR, chRCC, pRCC, CDC, SRC and benign kidney tumors (oncocytoma and AML) were grouped together, anticipating that changes in urine metabolite levels in tumor types would follow similar trends. The metabolic pathways associated with selected potential biomarkers of kidney cancer were evaluated by MetaboAnalyst software (version 4.0) using *Homo sapiens* (human) as library.

3. Results and discussion

3.1. Distinguishing between kidney cancer and control samples by ^{1}H NMR

In the current study, we recorded high-resolution 1D ^{1}H NMR spectra of 50 urine metabolite extracts from patients suffering from kidney cancer and from 50 healthy volunteers. Figure 1 presents a representative one-dimensional (1D) ^{1}H NMR spectrum of

metabolite mixtures extracted from a urine sample of a kidney cancer patient or a healthy control. In total, 52 metabolites were identified and quantified in each urine sample using ^{1}H NMR spectroscopy for metabolite profiling. Visual comparison of the NMR spectra revealed significant differences in individual metabolite levels between the urine samples of kidney cancer patients and healthy controls. Representative ^{1}H NMR spectra of serum samples from kidney cancer patients are shown in Figure 1, along with metabolites identified (Figure 1).

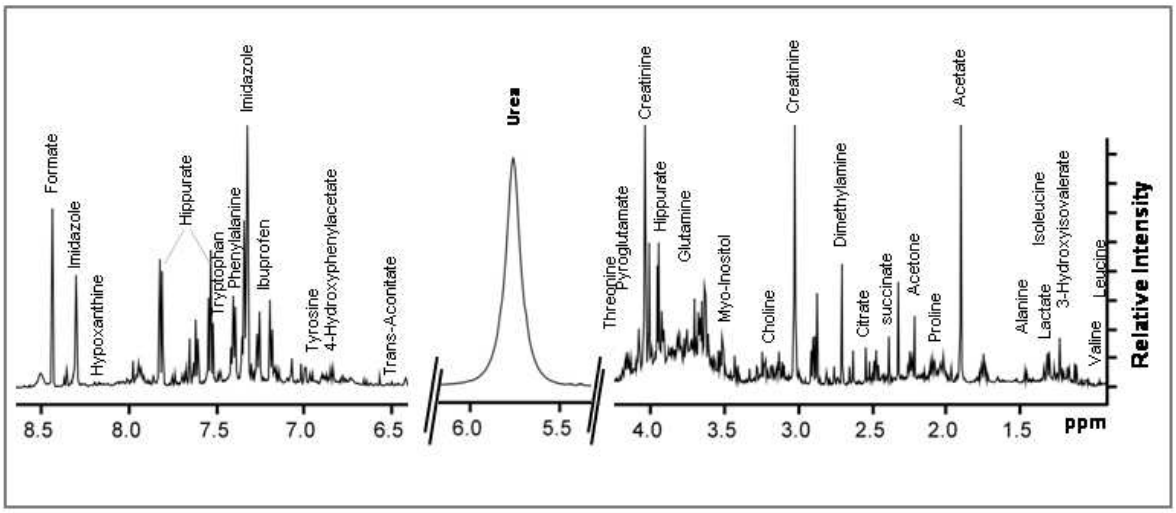

Figure 1. Characteristic 1D ^{1}H NMR spectrum of a protein-free metabolite extract mixture obtained from a urine sample of a kidney cancer patient, recorded on MSU 600 MHz (14 Tesla) solution NMR spectrometer. NMR signals assigned to specific metabolites using the Chenomx sofware are labeled. X-axis denotes 1H chemical shift (ppm) and y-axis indicates relative intensity of the NMR signals.

Univariate and multivariate statistical analyses of urinary metabolite patterns were employed to assess the discrimination accuracy between RCC and controls. These analyses also enabled to identify several significantly elevated levels of polar small molecules in kidney cancer (Supplementary material Table S1). Metabolite concentrations obtained by NMR were analyzed using principal component analysis (PCA) to evaluate whether the different patient versus control groups could be separated based on distinct metabolite profiles. The resulting 3D PCA scores plot (Figure 2 A) indicate that the metabolite profiles of cancer patients are to a large extent distinct from those of healthy controls, with PC1 and PC2 accounting for 35.4% and 8% of the variance, respectively. Group separations were further examined using supervised Partial Least Square-Discriminant Analysis, which revealed a clear separation between cancer patients and healthy controls, as shown in the 3D-PLSA scores plot of Figure 2B.

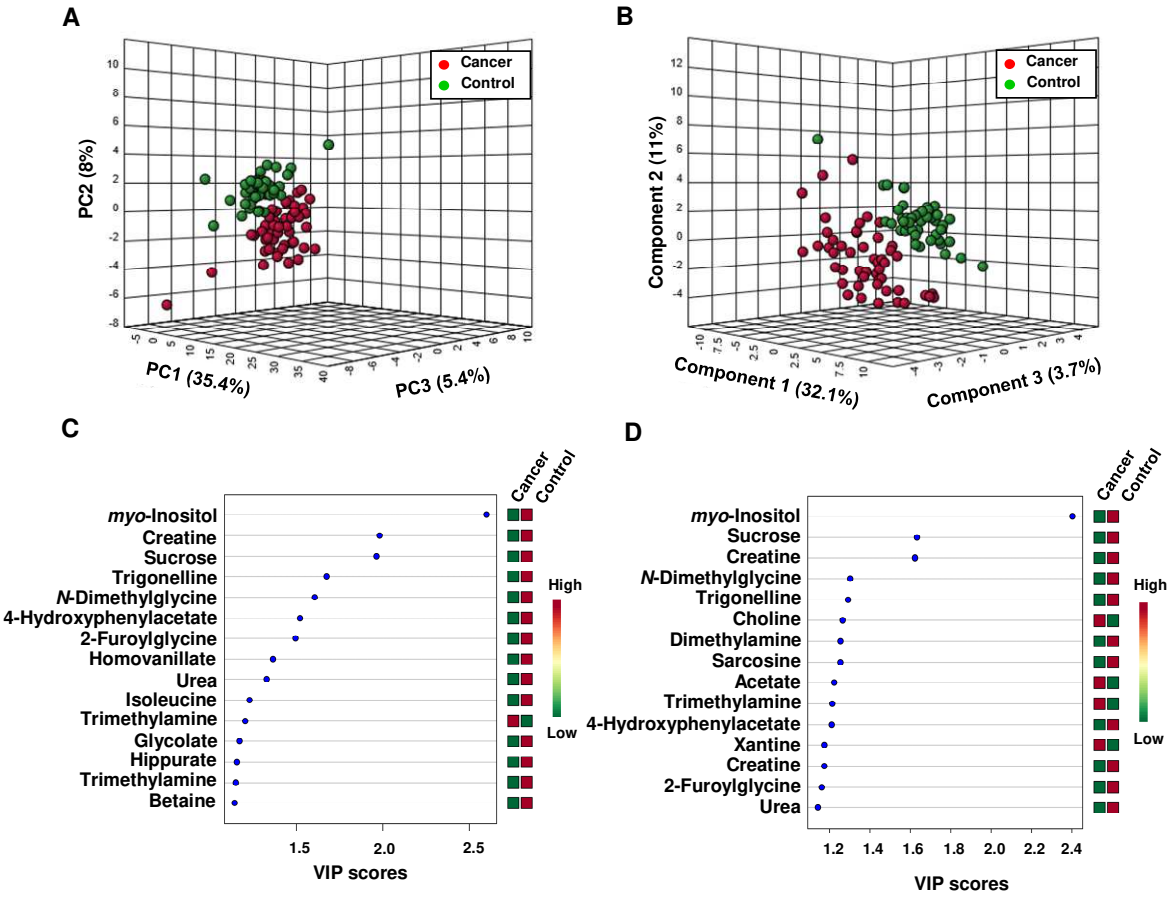

Figure 2. 2D-PCA scores plot generated from the NMR data of the urine cancer (red) and control (green) samples (A). 2D PLS-DA analysis of urine metabolite profiles identified by ^{1}H NMR (B). VIP scores ranking the most important metabolites (VIP > 1) that contributes to the separation in the PLS-DA analysis between cancer and control samples for component 1 (C) and for component 2 (D).

Good discrimination was observed between patients with kidney cancer and healthy control (R^2=0.85, Q^2=0.81, accuracy=0.99), revealing significant differences in urinary metabolic profiles (Figure S1, Supplementary material). Analysis of the variable importance in projection (VIP) scores of the PLS-DA model, combined with statistical test analysis (p values <5xE-4) indicate twenty metabolites responsible for differences (Figure 2, S1 and Table 1 in Supplementary material). In details, PLS-DA comparisons revealed higher level of trimethylamine and lower levels of myo-inositol, creatine, sucrose, trigonelline, *N*-dimethylglycine, 4-hydroxyphenylacetate, 2-furoylglycine, homovanillate, glycolate, Hippurate, and betaine when comparing the urine metabolite profiles of the cancer patients compared to healthy controls (Figure 2C).

Twenty metabolites were found to be statistically significant for discriminating between cancer patients and healthy controls, according to the criterion of a VIP value > 1, and FDR and adjusted p-value below 0.05. Metabolite profiles and concentration data for the complete set of 52 metabolites with mean concentration values and all relevant statistical parameters are reported in Table S1 (Supplementary material). Next, a multivariate Receiver Operating Characteristics (ROC) curve analysis was performed based on the differing concentrations of

these twenty selected metabolites to generate a better predictive model to discriminate the urine metabolite profiles of kidney cancer patients compared to controls. In our study, 12 significant metabolites with an area under the curve (AUC) threshold above 0.75 included myo-inositol, creatine, sucrose, trigonelline, 2-furoylglycine, urea, 4-hydroxyphenylacetate, alanine, homovanillate, glycolate, *N*-dimethylglycine and isoleucine (Table 1).

Table 1. Summary of fold concentration changes of potential metabolite markers, as revealed from ^{1}H NMR spectral analyses of urine metabolite samples from kidney cancer patients and healthy control volunteers

No.	Metabolite	AUC	VIP	P-value[a]	Fold change[b]					
					Cancer vs. Control	Benign vs. Control	Malignant vs. Control	G1 vs. Control	G2 vs. Control	G3 vs. Control
1	*myo*-Inositol	0.96	2.60	4.51E-40	0.03	0.00	0.03	0.00	0.02	0.00
2	Creatine	0.91	1.98	8.86E-16	0.19	0.24	0.18	0.15	0.23	0.14
3	Sucrose	0.86	1.96	2.05E-15	0.29	0.19	0.28	0.07	0.34	0.38
4	Trigonelline	0.86	1.67	1.20E-10	0.22	0.19	0.23	0.28	0.23	0.18
5	2-Furoylglycine	0.85	1.49	2.01E-08	0.32	0.38	0.30	0.52	0.27	0.21
6	Urea	0.83	1.33	9.96E-07	0.56	0.54	0.57	0.72	0.57	0.54
7	4-Hydroxyphenylacetate	0.82	1.52	1.02E-08	0.31	0.14	0.33	0.55	0.36	0.17
8	Alanine	0.81	1.09	8.20E-05	0.43	0.59	0.40	0.39	0.43	0.41
9	Homovanillate	0.81	1.36	4.48E-07	0.42	0.38	0.44	0.29	0.53	0.45
10	Glycolate	0.80	1.17	2.11E-05	0.51	0.59	0.50	0.45	0.46	0.61
11	*N*-Dimethylglycine	0.80	1.61	9.74E-10	0.47	0.49	0.47	0.43	0.46	0.49
12	Isoleucine	0.76	1.23	7.25E-06	0.55	0.86	0.51	0.27	0.50	0.68

[a]p-value determined from Student's t-test with Welch's correction; [b]calculated from the concentration mean values of cancer patients to control; G – grade of kidney cancer

Among these metabolites, the best ROC analysis results with the highest significance were achieved for the metabolite *myo*-inositol (AUC = 0.965, specificity= 1 and a sensibility = 1), followed by creatine (AUC = 0.911, specificity= 0.8 and a sensibility = 0.9), sucrose (AUC = 0.86, specificity=0.8 and a sensibility = 0.9), trigonelline (AUC = 0.856, specificity= 0.8 and a sensibility = 0.8) and 2-fluoroglycine (AUC = 0.853, specificity= 0.8 and a sensibility = 0.8). The range of concentrations for these individual metabolites in the urine samples of cancer patients compared to healthy controls is shown in Figure 3.

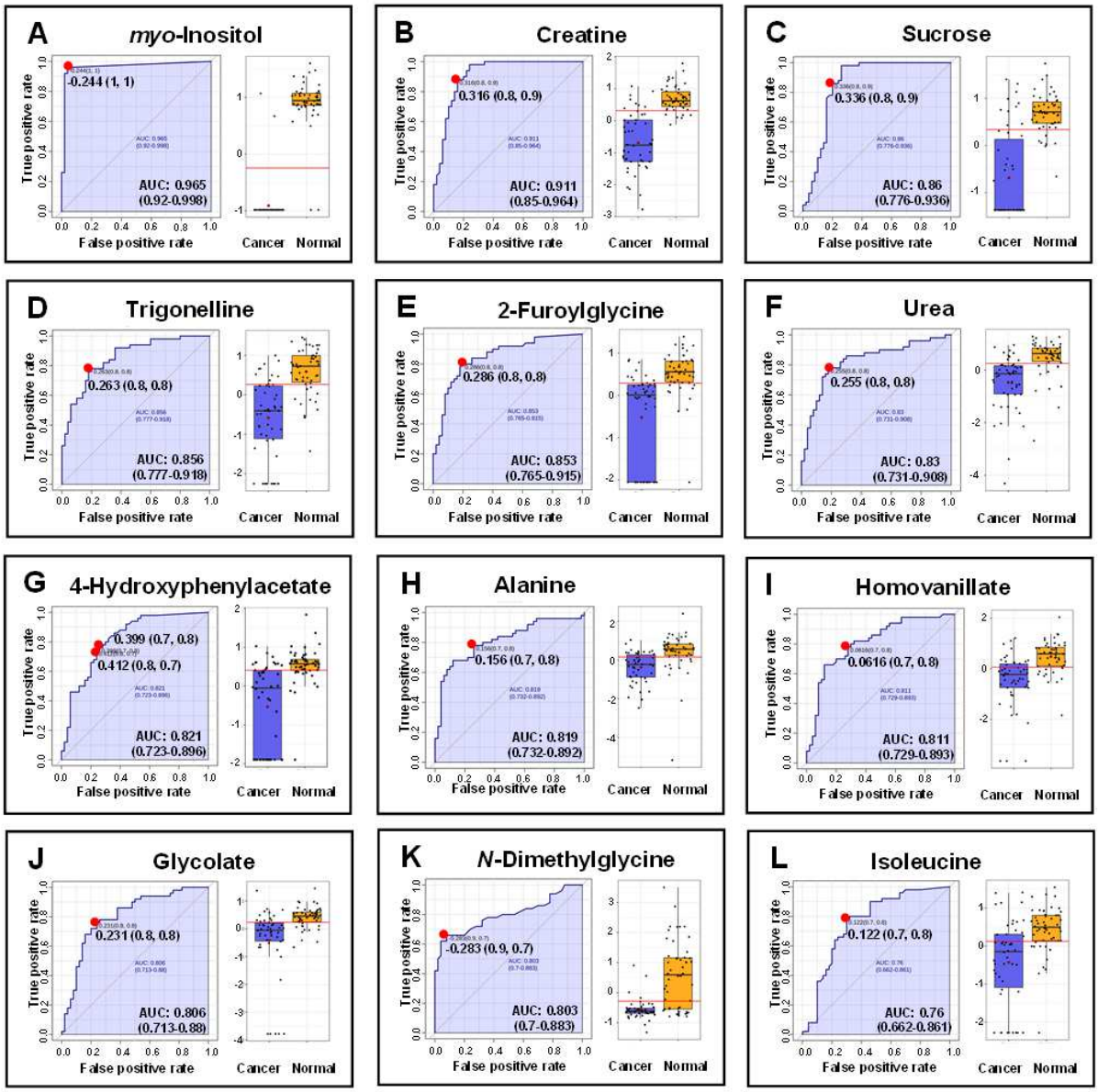

Figure 3. ROC curve analysis for potential biomarkers of kidney cancer predicted from univariate analysis. The left side of each panel indicates ROC curve for a particular metabolite, with 95% confidence interval (shadowed) and the solid red dot indicating the optimal cut-off associated with sensitivity and specificity values. The right side of each panel depicts the range of concentrations of each specific metabolite measured in the urine samples of kidney cancer patients and healthy controls. The horizontal red line in the graphs indicates the cut-off point.

Twelve metabolites exhibiting the highest AUC > 0.75 in the ROC curve generated (Figure S2, Supplementary material) were manually selected to construct a classifier in the random forest algorithm. An AUC of 0.986 with a confidence interval (CI) from 0.948 to 1 indicates a great sensitivity and specificity. This result suggests that the twelve specific metabolites presented above have the best predictive ability and could be used as diagnostic biomarkers to

distinguish urine samples from kidney cancer patients and control groups with high specificity and sensitivity.

3.2. Distinguishing between grade and type of kidney cancer in ^{1}H NMR dataset

^{1}H NMR metabolomics analysis of urine samples was further employed to evaluate whether distinct metabolic trends could distinguish between the different grades (grade 1-3) and types (benign and malignant) of kidney cancer tumors, and separate samples from cancer patients from the healthy control group. PCA scores plots showed practically no discrimination of benign from malignant and grade 1 from grade 2 and 3 (data not shown).
PLS-DA score plots shown in Figure 4A also did not reveal any significant trend correlated to tumor type. This suggests that metabolic patterns for those groups are not easily separable by just simply assessing differences in polar metabolite levels in urine samples. However, we obtained a good discrimination between these groups and controls, as indicated by the VIP score plots shown in Figures 4D and F. Comparing separately controls and cancer groups of varying type of tumors (controls vs benign and controls vs malignant) using PLS-DA analysis revealed a good discrimination between these groups (Figure 4). Quality factors for those models amounted to Q^2>0.77, R^2>0.85 and accuracy >0.98, with p values based on permutation tests smaller than 0.05. Detailed results are shown in supplementary material Figure S3. A variable importance plots revealed that *myo*-inositol and sucrose were significant contributors to the separation between controls vs malignant and controls vs benign. Trimethylamine presented the second biggest VIP value for the model when comparing benign types of cancer to healthy controls.

Analysis revealed higher differences of isoleucine and alanine levels in the model with malignant cancer compared to model with benign type of cancer (Table 1). This suggests that examining the differential levels of these metabolites may be an effective way to detect malignancy of the tumor in urine samples. An opposite trend was observed for 4-hydroxyphenylacetate.

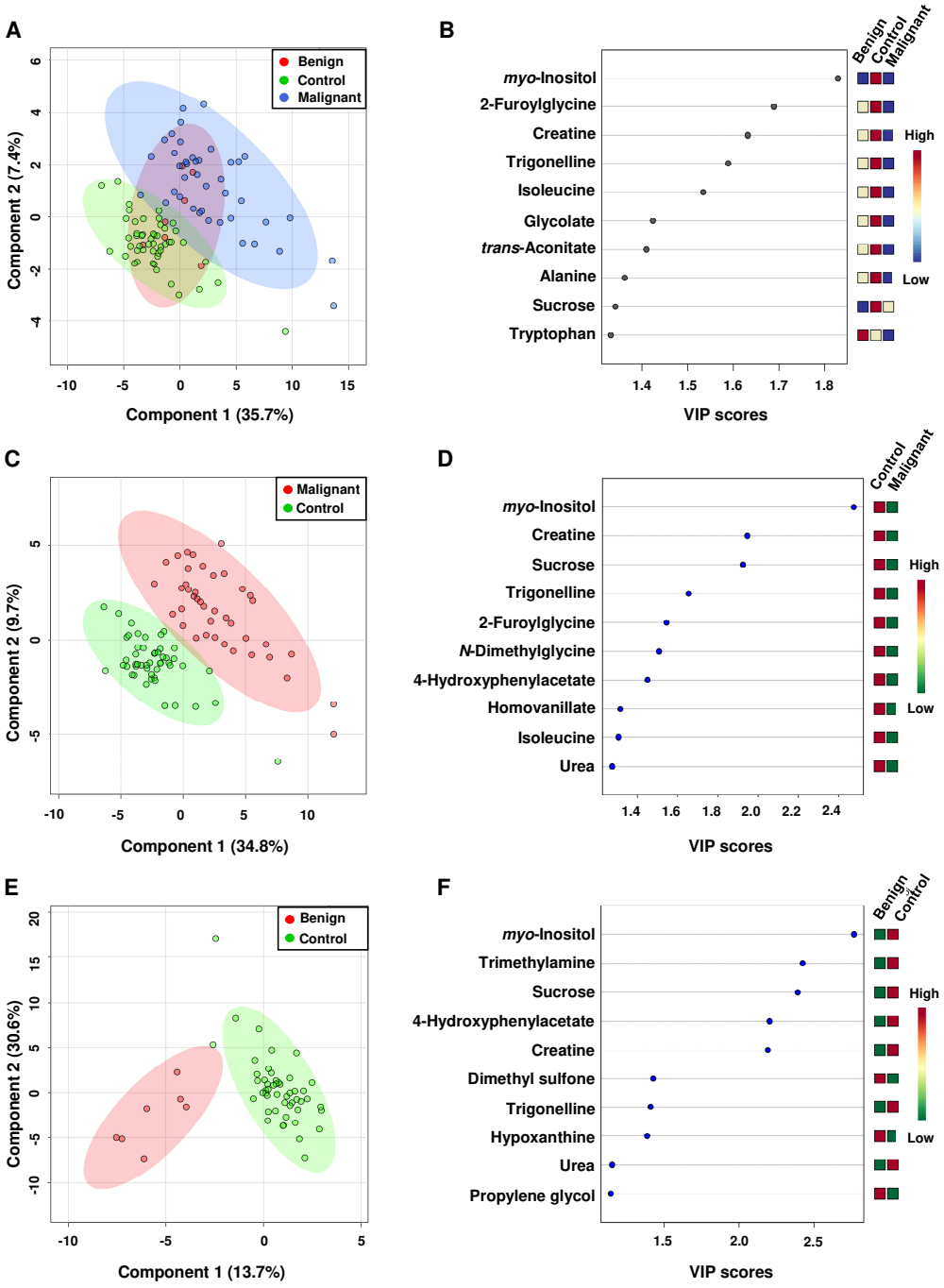

Figure 4. 2D-PLS DA analysis of NMR metabolite data of urine samples; (A) controls (green) compared with benign (red) and malignant (blue) patients and (B) the corresponding metabolite ranking according to VIP scores; (C) controls (green) compared with malignant (red) patients and (D) the corresponding metabolite ranking according to VIP scores; (E) controls (green) compared with benign (red) patients and (F) the corresponding metabolite ranking according to VIP scores;

PLS-DA score plots shown in Figure 5 reveal a good discrimination between controls and patients with different grade of kidney cancer (controls vs G1, controls vs G2 and controls vs G3). All three models met quality criteria (Q^2>0.72, R^2>0.90 and accuracy >0.99),

with p values based on permutation tests smaller than 0.05. Details of the model validation analyses are included in supplementary material Figure S4. Variable importance in projection (VIP) scores plots revealed that major metabolites responsible for group discrimination in all these models consisted of *myo*-inositol and creatine.

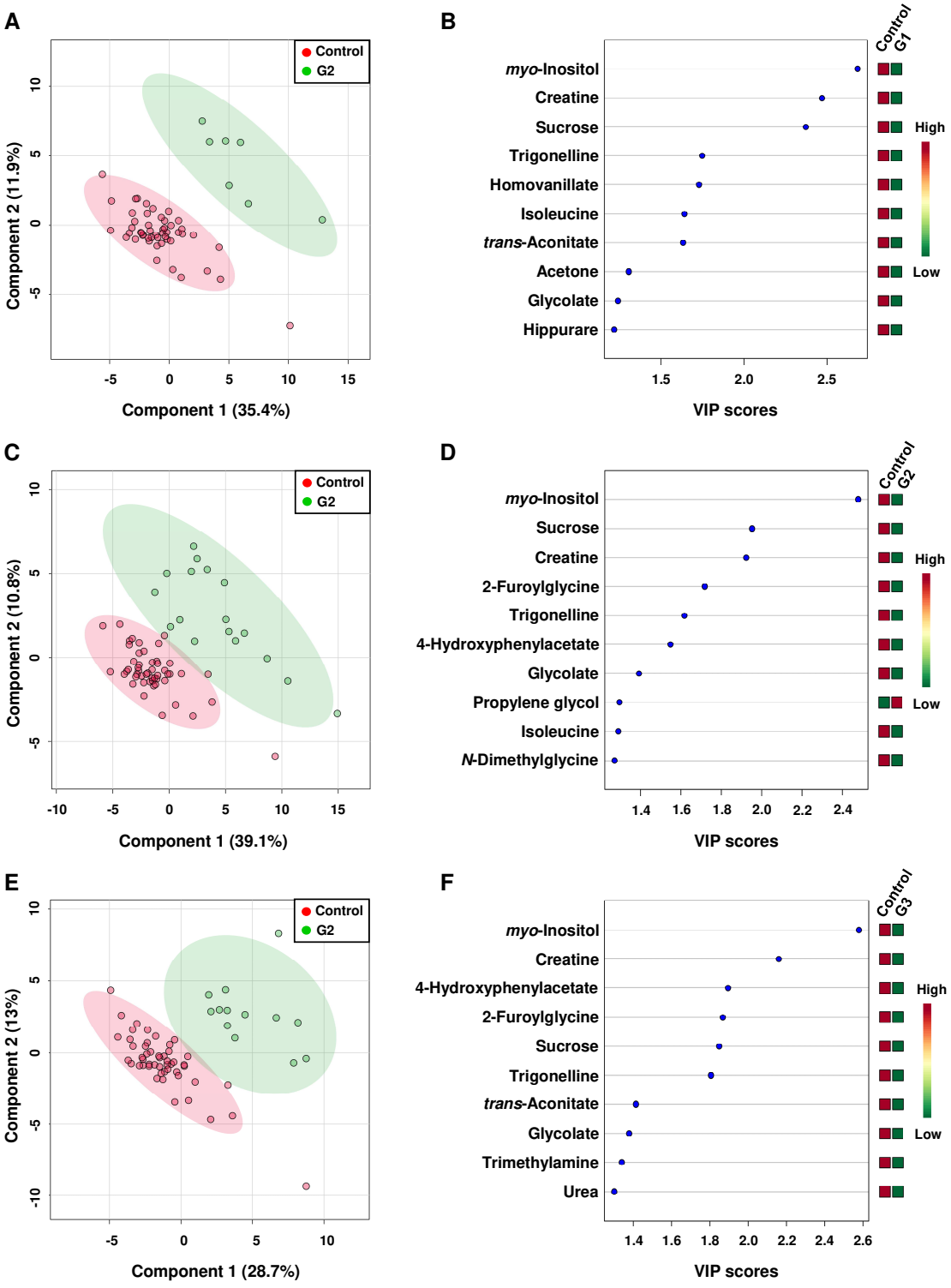

Figure 5. PLS DA analysis of NMR data of urine samples; (A) controls (red) compared with G1 (green) patients and; (C) controls (green) compared with G2 (red) patients; (E) controls

(green) compared with G3 (red) patients. Metabolite rankings according to VIP scores are shown in insets B, D and F for A, B and C analyses respectively.

Interestingly, analyses performed herein resulted in the identification of several metabolites that differentiate between cancer grades as shown in Table 2. Analysis of metabolite concentration changes revealed increasing levels of sucrose, glycolate, *N*-dimethylglycine and isoleucine with increasing tumor grade. The opposite trend was observed for trigonelline, 2-fluoroglycine, urea and 4-hydroxyphenylacetate (Table 1). All these observations confirmed that types and grades of kidney cancer have an influence on group discrimination, but only when cancer types and grades are analyzed separately from controls.

3.3. Metabolic profile of urine in kidney cancer with ^{109}AgNPET LDI MS

In this study, LDI MS-based approach was also applied to investigate the urine metabolic profiles of patients with kidney cancer. All spectra were recorded in positive ion mode due to high efficiency of cationization with the use of cationic nanoparticles. A number of 452 common features were detected in the urine samples of 50 patients with kidney cancer and 50 healthy controls, using ^{109}AgNPET LDI mass spectral analyses. The peak intensity data from LDI MS spectra was subjected to multivariate data analysis, and 2D-PCA and 2D-PLS-DA score plots were generated for the entire data set. 2D-PCA scores plots for mass spectral features showed poor discrimination of kidney cancer patients from controls (Figure 6A). Results from PLS-DA analysis as shown in Figure 6B highlight a clear separation between those two groups ($p = 0.029$, Figure S5, Supplementary material) with 120 features contributing to group separation (VIP > 1).

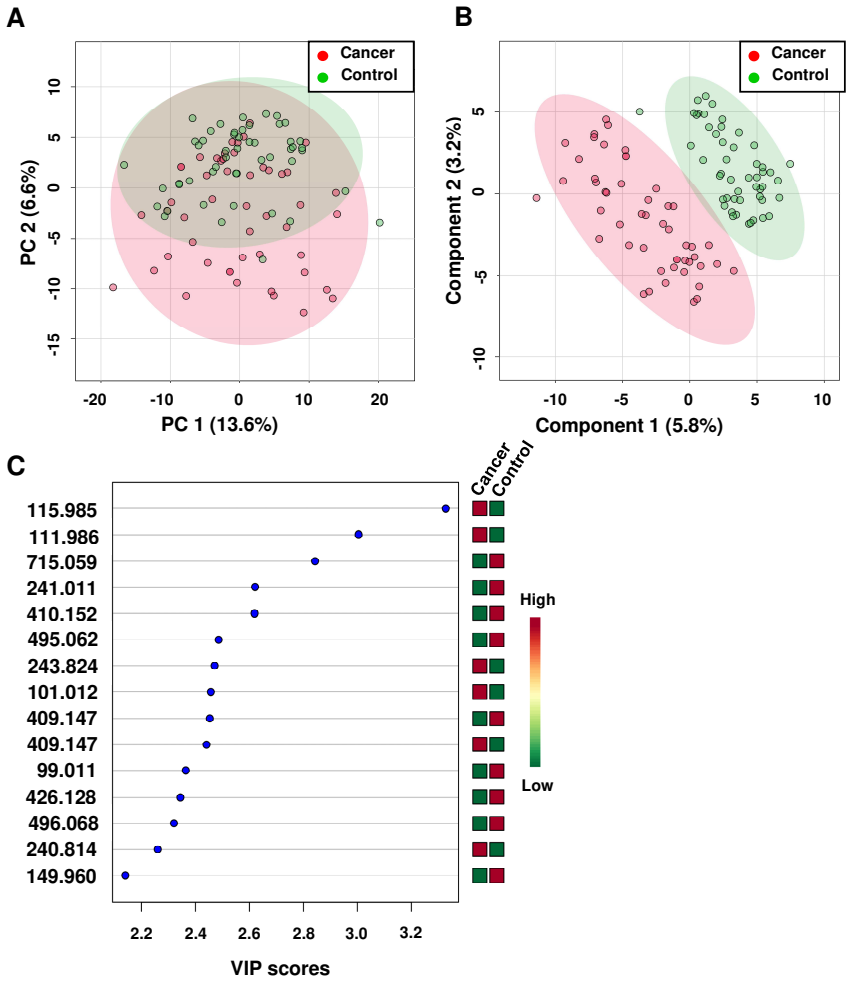

Figure 6. (A) 2D-PCA scores plot of kidney cancer and control group based on ^{109}AgNPET LDI MS metabolic profiles. (B) 2D-PLS-DA scores plot based on ^{109}AgNPET LDI MS. (C) Key first 15 MS features according to the VIP-parameter (>1). The colored boxes on the right indicate the relative concentrations of these metabolites in each group.

PLS-DA analyses of the LDI-MS metabolic profiles clearly show separated clusters in the 2D scores plots between the urine of kidney cancer patients and controls (Figure 6B) suggesting that the ^{109}AgNPET LDI MS-based urine metabolomics model can be used to identify the metabolic differences that separate these two groups. Validation and permutation tests (Figure S5, Supplementary material) showed that the PLS-DA model was reliable (Q^2 =0.52, and R^2 = 0.90; accuracy=0.87) and that the observed separation between the two groups is significant (p=0.029) (Figure S5, Supplementary material). To assess the potential of these *m/z* features to represent robust biomarkers of cancer phenotypes, VIP scores plots were employed to assess degree of importance (Figure 6C). Based on the individual VIPs, q- and p-values, 43 *m/z* features (*m/z* values) were found to be highly discriminatory between selected groups. Mean abundances of these significantly different *m/z* variables identified in the urine are reported in Table S4 (Supplementary material).

Table 2. Selected *m/z* values found in ^{109}AgNPET LDI MS spectra of urine from kidney cancer patients and control volunteers.

No.	*m/z*[a]	Putative metabolite	Adduct type	Mass error [ppm]	AUC	VIP	P-value[c]	FC[d]
1	241.011	Succinylacetoacetate	$[C_8H_{10}O_6+K]^+$	0.4	0.76	2.62	4.44E-06	0.44
2	425.120	Cys-Gly-Ser-His	$[C_{14}H_{22}N_6O_6S+Na]^+$	3.2	0.77	1.96	8.24E-04	0.46
3	495.062	His-Gly-Ser-Ser	$[C_{14}H_{22}N_6O_7+^{109}Ag]^+$	5.7	0.77	2.49	1.50E-05	0.51
4	496.068	Met-Thr-His	$[C_{15}H_{25}N_5O_5S+^{109}Ag]^+$	12.4	0.77	2.34	4.93E-05	0.46

[a]Experimental monoisotopic neutral mass; [b]Unknown; [c]p-value determined from Student's t-test with Welch's correction; [d]fold change between kidney cancer and healthy controls calculated as abundance mean value of cancer group divided by control group.

The *m/z* features were then used to search against four metabolite databases: HMDB, MetaCyc, LipidMaps, and Metlin to retrieve metabolites with similar masses. Unfortunately, only four urine features were putatively assigned to known metabolites. All of MS spectral features identified as being potentially good indicators of kidney cancer are reported in Table 2. Selected *m/z* values were further submitted to prediction model construction. ROC analysis indicated that seven *m/z* features have a strong diagnostic value to discriminate kidney cancer from controls, with AUC values above 0.75 (Table 2). Among the features, the most significant was observed for *m/z* 241.011, with an AUC value of 0.768, sensitivity of 0.7, and specificity of 0.7. The AUC resulting from the random forest algorithm was 0.83 within the range of 0.73 to 0.90 at the 95% confidence interval (CI) for 100-fold cross-validation (Figure S6, Supplementary material). The distribution in abundance of these mass spectral features in control and cancer urine samples is shown in Figure 7.

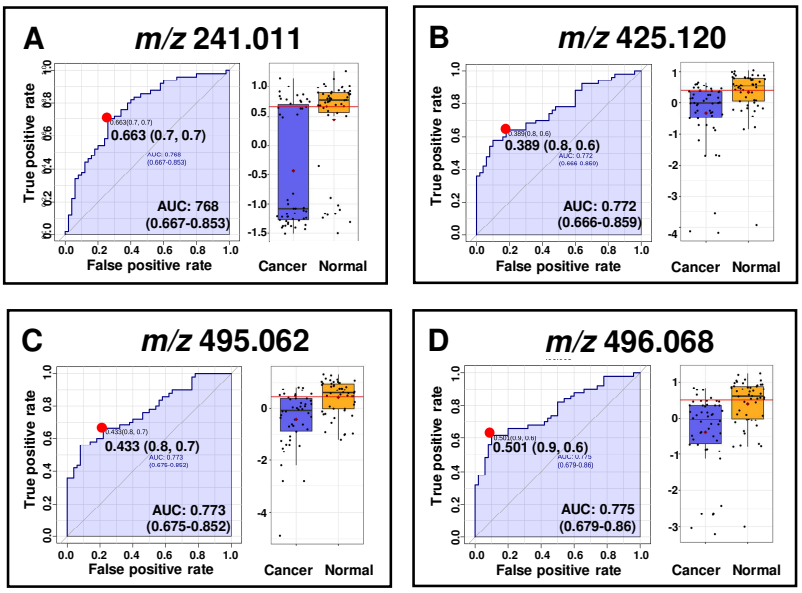

Figure 7. ROC curve analysis for mass spectral features representing potential biomarkers of kidney cancer. The left side of each panel represents the ROC curve of the select mass spectral features, with 95% confidence interval (shadowed) and the solid red dot indicates the optimal cut-off with the associated sensitivity and specificity values. The right side depicts abundance distribution in control and cancer samples with optimal cut-off as a horizontal dashed line.

Pathway analysis of biomarkers

The metabolic pathway analysis was applied to evaluation of the biological significance of potential biomarkers selected in the present study by significant changes (p-value< 0.05, FDR< 0.05 and VIP >1) using MetaboAnalyst 4.0 platform. The results demonstrated that four metabolic pathways, including galactose, glycine, serine and threonine metabolism, tyrosine metabolism and aminoacyl-tRNA biosynthesis were filtered out as the most important pathways related with the metabolic disturbances in patients with kidney cancer (Figure 8).

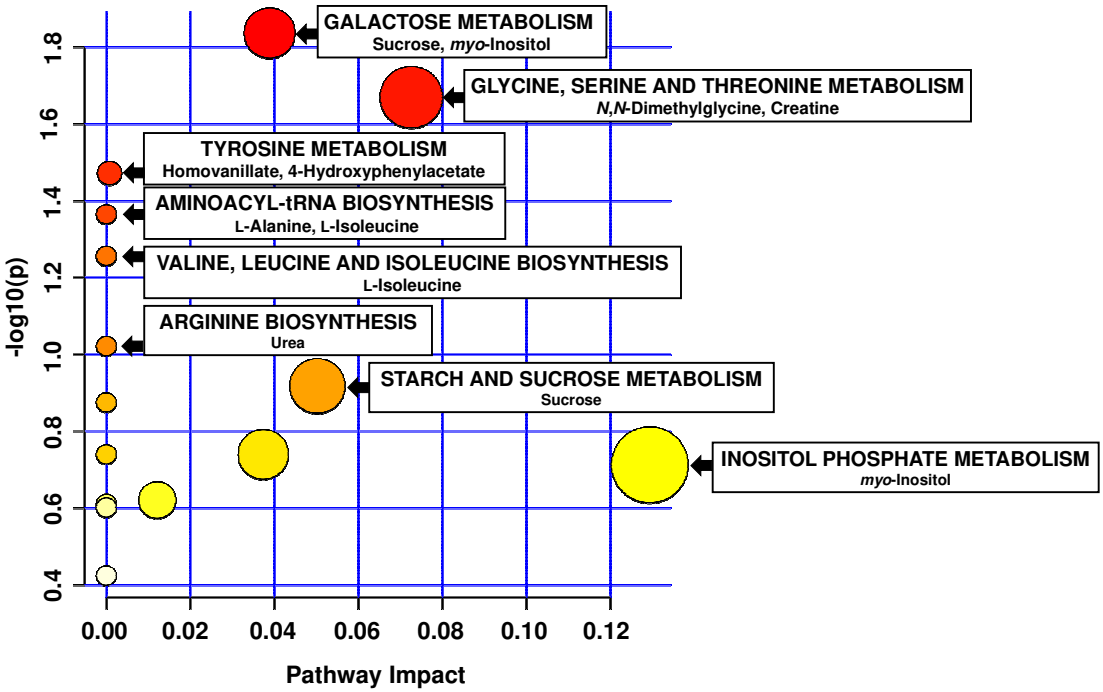

Figure 8. Summary of pathway analysis based on Kyoto Encyclopedia of Genes and Genomes (KEGG). A circle of darker color indicates a greater -log(p) value, and a circle of larger size indicates a greater pathway impact value.

Discussion

Body fluids such as blood and urine can be collected in a minimally invasive way for testing and thus are an excellent source of metabolite material. As shown in most diseases, changes in body metabolism are reflected in metabolite level changes of blood and urine.

In the current study, ^{1}H-NMR and LDI-MS-based approaches, together with multivariate statistical analysis, were applied to examine the urinary metabolome of kidney cancer patients and to identify potential diagnostic markers of this type of cancer. All selected potential urine biomarkers for kidney cancer have been compared to the previous reported studies in Table 3.

Table 3. Urine metabolites as potential biomarkers of kidney cancer finding in the current study compare to the previous reported studies

Name of metabolites	Sample Size			Technique	Tumor vs. Control		References number
	Total	Tumor	Control		Trend[a]	Fold change	
2-Furoylglycine	n=100	n=50	n=50	^{1}H NMR	↓	0.32	Our results
	n=129	n=61	n=68	LC-LTQ-Orbitrap MS	↑	2.09	Zhang et al. [23]
	n=62	n=29	n=33	UPLC-MS/MS	↓	-	Kim et al. [14]
4-Hydroxyphenylacetate	n=100	n=50	n=50	^{1}H NMR	↓	0.31	Our results
	n=91	n=42	n=49	^{1}H NMR	↓	-	Monteiro et al. [15]
	n=10	n=5	n=5	GC-TOF–MS	↓	0.80	Perroud et al. [12]
	n=62	n=29	n=33	UPLC-MS/MS	↓	-	Kim et al. [14]
Alanine	n=100	n=50	n=50	^{1}H NMR	↓	0.43	Our results
	n=62	n=29	n=33	UPLC-MS/MS	↓	-	Kim et al. [24]

	n=78	n=49	n=29	^{1}H NMR	↑	-	Ragone et al. [17]
Creatine	n=100	n=50	n=50	^{1}H NMR	↓	0.19	Our results
	n=91	n=42	n=49	^{1}H NMR	↓	-	Monteiro et al. [15]
	n=62	n=29	n=33	UPLC MS/MS	↓	0.90	Ganti et al. [11]
	n=78	n=49	n=29	^{1}H NMR	↑	-	Ragone et al. [17]
	n=62	n=29	n=33	UPLC-MS/MS	↑	1.14	Kim et al. [14]
Cys-Gly-Ser-His	n=100	n=50	n=50	^{109}AgNPET LDI MS	↓	0.46	Our results
Glycolate	n=100	n=50	n=50	^{1}H NMR	↓	0.51	Our results
His-Gly-Ser-Ser	n=100	n=50	n=50	^{1}H NMR	↓	0.51	Our results
Homovanillate	n=100	n=50	n=50	^{1}H NMR	↓	0.42	Our results
	n=62	n=29	n=33	UPLC-MS/MS	↓	-	Kim et. al.
Isoleucine	n=100	n=50	n=50	^{1}H NMR	↓	0.55	Our results
	n=62	n=29	n=33	UPLC-MS/MS	↓	-	Kim et al. [14]
	n=91	n=42	n=49	^{1}H NMR	↑	13.5	Monteiro et al. [15]
Met-Thr-His	n=100	n=50	n=50	^{1}H NMR	↓	0.46	Our results
myo-Inositol	n=100	n=50	n=50	^{1}H NMR	↓	0.03	Our results
	n=62	n=29	n=33	UPLC-MS/MS	↓	-	Kim et al. [14]
	n=10	n=5	n=5	GC-TOF–MS	↑	11.50	Perroud et al. [12]
N-Dimethylglycine	n=100	n=50	n=50	^{1}H NMR	↓	0.47	Our results
	n=62	n=29	n=33	UPLC-MS/MS	↓	-	Kim et al. [14]
Succinylacetoacetate	n=100	n=50	n=50	^{1}H NMR	↓	0.44	Our results
Sucrose	n=100	n=50	n=50	^{1}H NMR	↓	0.29	Our results
	n=10	n=5	n=5	GC-TOF–MS	↓	0.70	Perroud et al. [12]
	n=62	n=29	n=33	UPLC-MS/MS	↓	-	Kim et al. [14]
Trigonelline	n=100	n=50	n=50	^{1}H NMR	↓	0.22	Our results
	n=91	n=42	n=49	^{1}H NMR	↓	-	Monteiro et al. [15]
Urea	n=100	n=50	n=50	^{1}H NMR	↓	0.53	Our results
	n=62	n=29	n=33	UPLC-MS/MS	↓	-	Kim et al. [14]

[a]Metabolites with"↑ /↓ " means increased/decreased; GC-TOF–MS - gas chromatography/time-of-flight mass spectrometry; LC-LTQ-Orbitrap MS - liquid chromatography coupled with electrospray ionization hybrid linear trap quadrupole-Orbitrap mass spectrometry; UPLC-MS/MS - ultrahigh performance liquid chromatography/tandem mass spectrometry

Using 1D ^{1}H NMR metabolite profiling, we identified 12 metabolites whose level changes were discriminatory and could be used to differentiate between cancer patients and healthy controls, in a statistically significant manner. Interestingly, all of them were found in lower concentrations in the urine of patients with RCC compared to controls. An explanation for this phenomenon may be the impairment of normal kidney function by cancer, which reduces the excretion of metabolites into the urine. LDI-MS results suggest that seven *m/z* values could be used as diagnostic variables enabling the distinction between kidney cancer and the control groups with high specificity and sensitivity.

PCA, PLS-DA and random forest models were employed for the statistical analysis of the NMR and MS metabolomics data recorded. The greatest metabolite contribution to the PLS-DA models, expressed by VIP scores parameters, belongs to 4 substances: *myo*-inositol, creatine, sucrose, and trigonelline. These results are consistent with the study conducted by Popławski et.al, who also showed reduced levels of *myo*-insoitol, sucrose, urea, glycine and isoleucine in patients with RCC [25]. It is noteworthy that the mentioned authors analyzed concentration of metabolites in renal tissue, supporting the notion that changes in the

metabolism of kidney cells and tissues are reflected in the metabolite profiles of urine samples of cancer patients.

Highest AUC values - 0.96, 0.91, 0.86 and 0.86, which provide a measure of the test's ability to discriminate between healthy and cancer patients, corresponded to *myo*-inositol, creatine, sucrose and trigonelline, respectively. Those 4 metabolites were also characterized by the highest VIP score and lowest fold change.

In this study, a metabolite that best discriminated between cancer and control urine was myo-inositol. This compound mediates cell signal transduction and is a precursor of secondary messengers including inositol triphosphate and phosphatidylinositol. Kidney is the primary site of myo-inositol metabolism, where it is transformed into D-glucuronate by myo-inositol oxygenase [26]. We demonstrated that the mean level of myo-inositol is lower in the urine of cancer patients with RCC (FC=0.03), and that this metabolite most significantly discriminates between cancer and control (AUC=0.96). Down-regulation of inositol metabolism has been associated with the pathogenesis of various diseases, including cancer. *Myo*-inositol is suggested to exert anticancer activity by inhibition of the PI3K/Akt/mTOR pathway, which is a target for RCC therapy using mTOR inhibitors (temsirolimus, everolimus) [27].

Another metabolite which was found in lower concentration in the urine of cancer patients compared to controls is creatine. Creatine is primarily synthesized in the kidneys, and lower levels may be an indication of the altered ability of kidney cancer patients to synthesize this compound. In muscles, creatine is converted into creatinine, which is then excreted in the urine. Serum creatinine is a major marker of renal function. Muscle creatine plays a major role in a cellular energetic turnover which is achieved by transfer of the phosphate group of phosphocreatine to ADP to generate ATP. Our results are consistent with the study by Monteiro et. al. [15], which has suggested that reduced excretion of creatine in urine may be linked to reduced biosynthesis of guanidinoacetate, which is an intermediate of this pathway, and considered the rate-limiting step of creatine synthesis. Apart from creatinine, another important marker of kidney damage is urea. We observed reduced levels of urea in the urine of RCC patients, suggesting that these individuals may have impaired ability to excrete excess nitrogen via the urea cycle.

Similarly, to our study, Monteiro et. al. reported a decreased level of trigonelline in the urine of cancer patients. Trigonelline is an alkaloid, plant hormone, found in many plants including coffee beans. It is also synthesized endogenously by methylation of niacin (vitamin B_3). Lower trigonelline levels may thus be due to disturbances in nicotinate and nicotinamide metabolism. Moreover, Ragone et. al. reported that urine levels of creatine and trigonelline are lower in RCC patients before nephrectomy compared to the same patients after removing the tumor [28]. These observations are most likely due to the removal of the diseased kidney, which leads to reduced excretion of polar metabolites.

Another group of metabolites whose concentrations differ in the urine of kidney cancer patients compared to healthy controls is glycine and its derivatives. Glycine is a conditionally essential amino acid to the human diet, as it can be synthesized from serine. However, glycine biosynthesis is not sufficient to meet cellular metabolic needs, as it is involved in one-carbon metabolism (folate and methionine cycles) and generates precursors for various metabolic

pathways including lipids, nucleotides and proteins biosynthesis [29]. We observed lower concentrations of 2-furoylglycine (2-FG) and N-dimethylglycine (DMG) in the urine samples of RCC patients. DMG is an intermediate product of choline conversion to glycine, and an important intermediate of glycine metabolism. Monteiro et. al. reported a decreased level of glycine and dimethylglycine and an increased level of furoylglycine in the urine samples of cancer patients compared to those of healthy control [15]. Other amino acids whose concentrations are decreased in the urine of RCC patients include alanine and isoleucine. Reduced excretion of amino acids and their derivatives in urine may be caused by their use as precursors by rapidly dividing cancer cells, which use amino acids as substrates to synthesize new cellular components.

Using ^{109}AgNPET LDI MS metabolite profiling, we putatively identified 4 metabolites whose levels were significantly changed in cancer patients and healthy controls. In this study we observed decreased abundance of 3 peptides in the urine of the patients with renal cancer: Cys-Gly-Ser-His, His-Gly-Ser-Ser and Met-Thr-His. Numerous studies have shown the important role of amino acids metabolism in cancerogenesis. They are substrates for the synthesis of proteins, lipids, nucleotides and purines. Moreover, they are involved in gluconeogenesis and in the citric acid cycle, which is essential for cellular energetic turnover. [30]. Therefore, fast proliferating cancer cells have high demand for amino acids. Aforementioned tri and tetrapeptides contain histidine in their composition. It is an essential amino acid, thus cannot be synthesized in the human body and repletion is fully dependent on diet and bacterial microbiota in the intestines. This may explain decreased abundance of histidine-based polypeptides in the urine of the patients with RC, in comparison to control. Another metabolite downregulated in the urine of the patients with RCC is succinylacetoacetate. It belongs to the class of medium-chain keto acids. Elevated concentration in urine is observed in tyrosinemia type I, a rare genetic disorder of the tyrosine metabolism. It is a result of mutations in the both copies of the gene coding fumarylacetoacetate hydrolase (FAH) - enzyme that catalyzes conversion of fumarylacetoacetate to fumarate and acetoacetate. Absence of this enzyme results in accumulation of succinylacetoacetate and succinylacetone which are excreted in the urine. We observed decreased concentration of succinylacetoacetate in the urine of patients with RCC.

4. Conclusion

In present study, we evaluated the feasibility of using potential urine biomarkers to distinguish between kidney cancer patients and healthy controls. Metabolomics studies of polar metabolite profiles present in urine and based on high-resolution ^{1}H NMR and ^{109}AgNPET LDI MS, coupled with multivariate statistical analysis (PLS-DA), revealed candidate diagnostic metabolome differences between urine of patients with kidney cancer and healthy people. Altered levels of several urine metabolites were found to be significant and valuable discriminators of kidney cancer compared to healthy controls. Using a ^{1}H NMR metabolomics approach, twelve common metabolites were found to discriminate kidney cancer patients from healthy controls, and consisted of myo-inositol, creatine, sucrose,

trigonelline, 2-furoylglycine, urea, 4-hydroxyphenylacetate, alanine, homovanillate, glycolate, *N*-dimethylglycine and isoleucine. LDI MS analysis revealed an additional seven mass spectral features that could potentially be valuable biomarkers, four of which were putatively identified as specific metabolites. Several important endogenous compounds, whose levels were altered between patients and controls and which have interesting bioactive properties and pharmacological potential were discussed. The ^{1}H NMR based metabolomic approach was also successfully applied to discriminate between different types and grades of kidney cancer, separately from healthy controls. Lastly, this study has revealed that both NMR and MS have the potential to identify informative urine biomarkers of kidney cancer. Monitoring changes in urine metabolite levels could become a valuable avenue to screen and track kidney cancer disease progression, in a less invasive way to what is currently used to diagnose and follow kidney cancer patients' recovery from treatment.

Acknowledgements
Research was supported by National Science Centre (Poland), research project OPUS Number 2016/23/B/ST4/00062. ^{1}H NMR spectra were recorded at Montana State University-Bozeman on a cryoprobe-equipped 600 MHz (14 Tesla) AVANCE III solution NMR spectrometer housed in MSU's NMR Center. Funding for MSU NMR Center's NMR instruments has been provided in part by the NIH SIG program (1S10RR13878 and 1S10RR026659), the National Science Foundation (NSF-MRI:DBI-1532078), the Murdock Charitable Trust Foundation (2015066:MNL), and support from the office of the Vice President for Research, Economic Development, and Graduate Education at MSU.

Competing interests
The authors declare no competing financial and/or non-financial interests.

Data Availability Statement
The data that support the findings of this study are available from the corresponding author upon reasonable request.

Author contributions
Conceptualization: T.R., J.N.; Methodology: J.N., T.R.; Formal analysis: J.N., T.R.; Investigation: J.N., T.R.; Resources: K.O., T.R., B.T.; V.C.; Data Curation: V.C., B.T., J.N., A.A.; Writing - Original Draft: J.N., K.O.; Writing - Review & Editing: J.N., T.R., V.C., B.T.; Visualization: J.N.; Supervision: T.R., V.C., B.T.; Project Administration: T.R.; Funding acquisition: T.R., V.C., B.T.

References

[1] J.J. Hsieh, M.P. Purdue, S. Signoretti, C. Swanton, L. Albiges, M. Schmidinger, D.Y. Heng, J. Larkin, V. Ficarra, Renal cell carcinoma (RCC) encompasses a heterogeneous group of cancers derived from renal tubular epithelial cells, Nat. Publ. Gr. 3 (2017). doi:10.1038/nrdp.2017.9.

[2] A. Thorstenson, M. Bergman, A.H. Scherman-Plogell, S. Hosseinnia, B. Ljungberg, J. Adolfsson, S. Lundstam, Tumour characteristics and surgical treatment of renal cell carcinoma in Sweden 2005-2010: A population-based study from the National Swedish Kidney Cancer Register, Scand. J. Urol. 48 (2014) 231–238. doi:10.3109/21681805.2013.864698.
[3] B.S. Sanganeria, R. Misra, K.K. Shukla, Molecular Diagnostics in Renal Cancer, in: Mol. Diagnostics Cancer Patients, Springer Singapore, Singapore, 2019: pp. 199–218. doi:10.1007/978-981-13-5877-7_13.
[4] S.S. Dinges, A. Hohm, L.A. Vandergrift, J. Nowak, P. Habbel, I.A. Kaltashov, L.L. Cheng, Cancer metabolomic markers in urine: evidence, techniques and recommendations, Nat. Rev. Urol. 16 (2019) 339–362. doi:10.1038/s41585-019-0185-3.
[5] L. Lin, Z. Huang, Y. Gao, Y. Chen, W. Hang, J. Xing, X. Yan, LC-MS-based serum metabolic profiling for genitourinary cancer classification and cancer type-specific biomarker discovery, Proteomics. 12 (2012) 2238–2246. doi:10.1002/pmic.201200016.
[6] B.B. Misra, R.P. Upadhayay, L.A. Cox, M. Olivier, Optimized GC–MS metabolomics for the analysis of kidney tissue metabolites, Metabolomics. 14 (2018). doi:10.1007/s11306-018-1373-5.
[7] H. Gao, B. Dong, J. Jia, H. Zhu, C. Diao, Z. Yan, Y. Huang, X. Li, Application of ex vivo 1H NMR metabonomics to the characterization and possible detection of renal cell carcinoma metastases, J. Cancer Res. Clin. Oncol. 138 (2012) 753–761. doi:10.1007/s00432-011-1134-6.
[8] R. Hájek, M. Lísa, M. Khalikova, R. Jirásko, E. Cífková, V. Študent, D. Vrána, L. Opálka, K. Vávrová, M. Matzenauer, B. Melichar, M. Holčapek, HILIC/ESI-MS determination of gangliosides and other polar lipid classes in renal cell carcinoma and surrounding normal tissues, Anal. Bioanal. Chem. 410 (2018) 6585–6594. doi:10.1007/s00216-018-1263-8.
[9] F. Süllentrop, D. Moka, S. Neubauer, G. Haupt, U. Engelmann, J. Hahn, H. Schicha, 31P NMR spectroscopy of blood plasma: Determination and quantification of phospholipid classes in patients with renal cell carcinoma, NMR Biomed. 15 (2002) 60–68. doi:10.1002/nbm.758.
[10] F. Zhang, X. Ma, H. Li, G. Guo, P. Li, H. Li, L. Gu, X. Li, L. Chen, X. Zhang, The predictive and prognostic values of serum amino acid levels for clear cell renal cell carcinoma, Urol. Oncol. Semin. Orig. Investig. 35 (2017) 392–400. doi:10.1016/j.urolonc.2017.01.004.
[11] S. Ganti, S.L. Taylor, K. Kim, C.L. Hoppel, L. Guo, J. Yang, C. Evans, R.H. Weiss, Urinary acylcarnitines are altered in human kidney cancer, Int. J. Cancer. 130 (2012) 2791–2800. doi:10.1002/IJC.26274.
[12] B. Perroud, J. Lee, N. Valkova, A. Dhirapong, P.-Y. Lin, O. Fiehn, D. Kültz, R.H. Weiss, Pathway analysis of kidney cancer using proteomics and metabolic profiling, Mol. Cancer. 5 (2006) 64. doi:10.1186/1476-4598-5-64.
[13] T. Kind, V. Tolstikov, O. Fiehn, R.H. Weiss, A comprehensive urinary metabolomic approach for identifying kidney cancerr, Anal. Biochem. 363 (2007) 185–195. doi:10.1016/j.ab.2007.01.028.
[14] K. Kim, S.L. Taylor, S. Ganti, L. Guo, M. V. Osier, R.H. Weiss, Urine metabolomic analysis identifies potential biomarkers and pathogenic pathways in kidney cancer, Omi. A J. Integr. Biol. 15 (2011) 293–303. doi:10.1089/omi.2010.0094.
[15] M.S. Monteiro, A.S. Barros, J. Pinto, M. Carvalho, A.S. Pires-Luís, R. Henrique, C. Jerónimo, M.D.L. Bastos, A.M. Gil, P. Guedes De Pinho, Nuclear Magnetic Resonance metabolomics reveals an excretory metabolic signature of renal cell carcinoma, Sci.

Rep. 6 (2016) 1–14. doi:10.1038/srep37275.
[16] H. Gao, B. Dong, X. Liu, H. Xuan, Y. Huang, D. Lin, Metabonomic profiling of renal cell carcinoma: High-resolution proton nuclear magnetic resonance spectroscopy of human serum with multivariate data analysis, Anal. Chim. Acta. 624 (2008) 269–277. doi:10.1016/j.aca.2008.06.051.
[17] R. Ragone, F. Sallustio, S. Piccinonna, M. Rutigliano, G. Vanessa, S. Palazzo, G. Lucarelli, P. Ditonno, M. Battaglia, F. Fanizzi, F. Schena, Renal Cell Carcinoma: A Study through NMR-Based Metabolomics Combined with Transcriptomics, Diseases. 4 (2016) 7. doi:10.3390/diseases4010007.
[18] J. Nizioł, W. Rode, B. Laskowska, T. Ruman, Novel Monoisotopic ^{109} AgNPET for Laser Desorption/Ionization Mass Spectrometry, Anal. Chem. 85 (2013) 1926–1931. doi:10.1021/ac303770y.
[19] J. Nizioł, W. Rode, B. Laskowska, T. Ruman, Novel monoisotopic ^{109}AgNPET for laser desorption/ionization mass spectrometry, Anal. Chem. 85 (2013). doi:10.1021/ac303770y.
[20] A.L. Fuchs, S.M. Schiller, W.J. Keegan, M.C.B. Ammons, B. Eilers, B. Tripet, V. Copié, Quantitative 1H NMR Metabolomics Reveal Distinct Metabolic Adaptations in Human Macrophages Following Differential Activation, Metabolites. 9 (2019) 248. doi:10.3390/metabo9110248.
[21] A.H. Emwas, E. Saccenti, X. Gao, R.T. McKay, V.A.P.M. dos Santos, R. Roy, D.S. Wishart, Recommended strategies for spectral processing and post-processing of 1D 1 H-NMR data of biofluids with a particular focus on urine, Metabolomics. 14 (2018). doi:10.1007/s11306-018-1321-4.
[22] J. Chong, D.S. Wishart, J. Xia, Using MetaboAnalyst 4.0 for Comprehensive and Integrative Metabolomics Data Analysis, Curr. Protoc. Bioinforma. 68 (2019). doi:10.1002/cpbi.86.
[23] M. Zhang, X. Liu, X. Liu, H. Li, W. Sun, Y. Zhang, A pilot investigation of a urinary metabolic biomarker discovery in renal cell carcinoma, Int. Urol. Nephrol. 52 (2020) 437–446. doi:10.1007/s11255-019-02332-w.
[24] K. KIm, P. Aronov, S.O. Zakharkin, D. Anderson, B. Perroud, I.M. Thompson, R.H. Weiss, Urine metabolomics analysis for kidney cancer detection and biomarker discovery, Mol. Cell. Proteomics. 8 (2009) 558–570. doi:10.1074/mcp.M800165-MCP200.
[25] P. Popławski, T. Tohge, J. Bogusławska, B. Rybicka, Z. Tański, V. Treviño, A.R. Fernie, A. Piekiełko-Witkowska, Integrated transcriptomic and metabolomic analysis shows that disturbances in metabolism of tumor cells contribute to poor survival of RCC patients, Biochim. Biophys. Acta - Mol. Basis Dis. 1863 (2017) 744–752. doi:10.1016/j.bbadis.2016.12.011.
[26] H.H. Chang, H.N. Chao, C.S. Walker, S.Y. Choong, A. Phillips, K.M. Loomes, Renal depletion of myo-inositol is associated with its increased degradation in animal models of metabolic disease, Am. J. Physiol. - Ren. Physiol. 309 (2015) F755–F763. doi:10.1152/ajprenal.00164.2015.
[27] M. Bizzarri, S. Dinicola, A. Bevilacqua, A. Cucina, Broad Spectrum Anticancer Activity of Myo-Inositol and Inositol Hexakisphosphate, (2016). doi:10.1155/2016/5616807.
[28] R. Ragone, F. Sallustio, S. Piccinonna, M. Rutigliano, G. Vanessa, S. Palazzo, G. Lucarelli, P. Ditonno, M. Battaglia, F.P. Fanizzi, F.P. Schena, Renal Cell Carcinoma: A Study through NMR-Based Metabolomics Combined with Transcriptomics, (n.d.). doi:10.3390/diseases4010007.
[29] J.W. Locasale, Serine, glycine and one-carbon units: cancer metabolism in full circle,

Nat. Rev. Cancer. 13 (2013) 572–583. doi:10.1038/nrc3557.
[30] E.L. Lieu, T. Nguyen, S. Rhyne, J. Kim, Amino acids in cancer, Exp. Mol. Med. 52 (2020) 15–30. doi:10.1038/s12276-020-0375-3.